*The following resources related to this article are available online at www.sciencemag.org*
*(this information is current as of November 12, 2010 ):*

**Updated information and services,** including high-resolution figures, can be found in the online version of this article at:
http://www.sciencemag.org/cgi/content/full/324/5934/1540

**Supporting Online Material** can be found at:
http://www.sciencemag.org/cgi/content/full/324/5934/1540/DC1

This article **cites 8 articles**, 1 of which can be accessed for free:
http://www.sciencemag.org/cgi/content/full/324/5934/1540#otherarticles

This article has been **cited by** 6 article(s) on the ISI Web of Science.

This article appears in the following **subject collections**:
Astronomy
http://www.sciencemag.org/cgi/collection/astronomy

4. P. V. Nguyen, T. Abel, E. R. Kandel, *Science* **265**, 1104 (1994).
5. K. C. Martin *et al.*, *Cell* **91**, 927 (1997).
6. U. Frey, R. G. Morris, *Nature* **385**, 533 (1997).
7. A. Casadio *et al.*, *Cell* **99**, 221 (1999).
8. K. C. Martin, *Curr. Opin. Neurobiol.* **14**, 305 (2004).
9. M. A. Sutton, E. M. Schuman, *Cell* **127**, 49 (2006).
10. A. Govindarajan, R. J. Kelleher, S. Tonegawa, *Nat. Rev. Neurosci.* **7**, 575 (2006).
11. O. Steward, W. B. Levy, *J. Neurosci.* **2**, 284 (1982).
12. L. E. Ostroff, J. C. Fiala, B. Allwardt, K. M. Harris, *Neuron* **35**, 535 (2002).
13. S. J. Tang *et al.*, *Proc. Natl. Acad. Sci. U.S.A.* **99**, 467 (2002).
14. J. Eberwine, B. Belt, J. E. Kacharmina, K. Miyashiro, *Neurochem. Res.* **27**, 1065 (2002).
15. R. Moccia *et al.*, *J. Neurosci.* **23**, 9409 (2003).
16. J. Zhong, T. Zhang, L. M. Bloch, *BMC Neurosci.* **7**, 17 (2006).
17. M. M. Poon, S. H. Choi, C. A. Jamieson, D. H. Geschwind, K. C. Martin, *J. Neurosci.* **26**, 13390 (2006).
18. T. Suzuki, Q. B. Tian, J. Kuromitsu, T. Kawai, S. Endo, *Neurosci. Res.* **57**, 61 (2007).
19. H. Kang, E. M. Schuman, *Science* **273**, 1402 (1996).
20. K. M. Huber, J. C. Roder, M. F. Bear, *J. Neurophysiol.* **86**, 321 (2001).
21. G. Aakalu, W. B. Smith, N. Nguyen, C. Jiang, E. M. Schuman, *Neuron* **30**, 489 (2001).
22. C. Job, J. Eberwine, *Nat. Rev. Neurosci.* **2**, 889 (2001).
23. W. Ju *et al.*, *Nat. Neurosci.* **7**, 244 (2004).
24. K. F. Raab-Graham, P. C. Haddick, Y. N. Jan, L. Y. Jan, *Science* **314**, 144 (2006).
25. V. F. Castellucci, S. Schacher, *Prog. Brain Res.* **86**, 105 (1990).
26. S. L. Mackey *et al.*, *Proc. Natl. Acad. Sci. U.S.A.* **84**, 8730 (1987).
27. V. Lyles, Y. Zhao, K. C. Martin, *Neuron* **49**, 349 (2006).
28. D. L. Glanzman, E. R. Kandel, S. Schacher, *Neuron* **3**, 441 (1989).
29. J. F. Brunet, E. Shapiro, S. A. Foster, E. R. Kandel, Y. Iino, *Science* **252**, 856 (1991).
30. J. Y. Hu, Y. Chen, S. Schacher, *J. Neurosci.* **27**, 11712 (2007).
31. J. Y. Hu, F. Wu, S. Schacher, *J. Neurosci.* **26**, 1026 (2006).
32. N. G. Gurskaya *et al.*, *Nat. Biotechnol.* **24**, 461 (2006).
33. Materials and methods are available as supporting material on *Science* Online.
34. K. Liu, J. Y. Hu, D. Wang, S. Schacher, *J. Neurobiol.* **56**, 275 (2003).
35. Z. Guan *et al.*, *Cell* **111**, 483 (2002).
36. L. Santarelli, P. Montarolo, S. Schacher, *J. Neurobiol.* **31**, 297 (1996).
37. D. Cai, S. Chen, D. L. Glanzman, *Curr. Biol.* **18**, 920 (2008).
38. We thank S. Braslow and K. Cadenas for assistance with image analysis; R. Grambo for assistance with figures; D. Black, C. Heusner, E. Meer, and L. Zipursky for critical reading of the manuscript; and G. Weinmaster and Martin laboratory members for helpful discussions. This work was supported by NIH grant NS045324, a W. M. Keck Foundation Young Scholar Award and Eleanor Leslie Term Chair from the UCLA Brain Research Institute (to K.C.M.), Canadian Institute of Health Research grant MT-15121 (to W.S.S.), and a fellowship from the Nakajima Foundation (to S.K.M.).

# REPORTS

# Solar-Like Oscillations in a Massive Star

Kévin Belkacem,[1,2]* Réza Samadi,[1] Marie-Jo Goupil,[1] Laure Lefèvre,[1] Fréderic Baudin,[3] Sébastien Deheuvels,[1] Marc-Antoine Dupret,[1,2] Thierry Appourchaux,[3] Richard Scuflaire,[2] Michel Auvergne,[1] Claude Catala,[1] Eric Michel,[1] Andrea Miglio,[2] Josefina Montalban,[2] Anne Thoul,[2] Suzanne Talon,[4] Annie Baglin,[1] Arlette Noels[2]

Seismology of stars provides insight into the physical mechanisms taking place in their interior, with modes of oscillation probing different layers. Low-amplitude acoustic oscillations excited by turbulent convection were detected four decades ago in the Sun and more recently in low-mass main-sequence stars. Using data gathered by the Convection Rotation and Planetary Transits mission, we report here on the detection of solar-like oscillations in a massive star, V1449 Aql, which is a known large-amplitude (β Cephei) pulsator.

Stars burn hydrogen into helium through nuclear fusion during most of their life. Once the central hydrogen gets exhausted, the helium core starts contracting, and hydrogen-shell burning takes over as the main energy source. The subsequent evolution depends mostly on a star's mass at birth but also on the physical mechanisms occurring during the hydrogen-burning phase. For instance, transport of chemical elements determines the helium core size, which is crucial for the evolution of stars. Transport pro-

cesses such as turbulence and those induced by rotation are not fully understood and are still poorly modeled, but stellar seismology can pro-

vide important constraints provided that the modes that probe the relevant regions are excited, detected, and identified. This will be the case for stars oscillating over a large range of oscillation modes probing different layers of the star.

Here, we report on the detection of solar-like oscillations (high-frequency acoustic modes that are damped but excited by turbulent convection and probe superficial convective regions) in a 10–solar mass star, V1449 Aql, already known to be a β Cephei (it oscillates on unstable low-frequency modes of high amplitude, also referred to as opacity-driven modes, which probe the deepest regions of stars) (*1*).

The largest-amplitude mode in the Fourier spectrum of V1449 Aql has been detected from the ground (*1*, *2*) at a frequency of 63.5 μHz. Those pulsations are excited by a thermal instability known as the κ-mechanism (*3*), which in the present case is related to the existence of an iron-opacity bump located in the upper layers of massive stars. The

**Fig. 1.** Fourier spectrum of prewhitened light curve obtained from the quasi-uninterrupted 150 days of observations, with a duty cycle of 90%, of the star V1449 Aql by CoRoT, showing structures that are reproduced over the 100- to 250-μHz interval. (**Inset**) Enlarged part of the spectrum showing a typical solar-like structure. Below 100 μHz, we enter the bulk regime of unstable modes (fig. S1), and the possible existence of many such modes
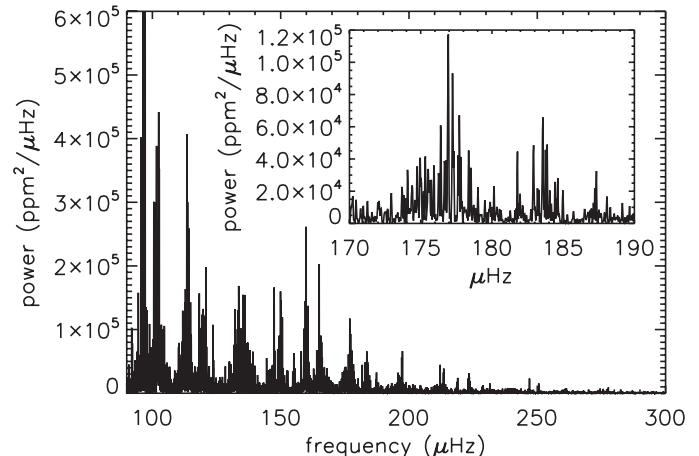


in this frequency domain then makes the deciphering of unstable versus stable modes quite delicate. Hence, to remain conservative we restrict the discussion to frequencies above 100 μHz.

[1]Laboratoire d'Études Spatiales et d'Instrumentation en Astrophysique, CNRS (UMR 8109), Observatoire de Paris, Place J. Janssen, F- 92195 Meudon, France; associated with Université Pierre et Marie Curie and Université Denis Diderot. [2]Institut d'Astrophysique et de Géophysique de l'Université de Liège, Allée du 6 Août 17–B 4000 Liège, Belgium. [3]Institut d'Astrophysique Spatiale, Université Paris-Sud 11 and CNRS (UMR 8617), Batiment 121, F-91405 Orsay, France. [4]Réseau Québécois de Calcul de Haute Performance, Université de Montréal, Casier Postal 6128, Succursale Centre-ville, Montréal, Québec H3C 3J8, Canada.

*To whom correspondence should be addressed. E-mail: kevin.belkacem@ulg.ac.be

iron-opacity bump in such a massive star induces the existence of a convective zone in the upper layers (4), which could be responsible for the excitation of the detected modes.

Our results are based on the quasi-uninterrupted (meaning, a duty cycle of 90%) light curve obtained over 150 days with the Convection Rotation and Planetary Transits (CoRoT) (5–7) Centre National d'Etudes Spatiales (CNES) space mission (Fig. 1). The dominant opacity-driven mode is located at 63.5 μHz with an amplitude of $3.9 \times 10^4$ parts per million (ppm). We looked for stochastically excited modes with frequencies above 100 μHz; below this limit, the existence of several opacity-driven modes makes the analysis more difficult. No signal is found above 250 μHz. In the frequency range 100 to 250 μHz, there are broad structures with a width of several μHz, with low amplitudes of hundreds of parts per million and well above the noise level, which is around 1 ppm.

These structures are not the result of instrumental effects [supporting online material (SOM) text]. To verify that they are not related to the existence of the opacity-driven modes, we carried out prewhitening (SOM text), which suppresses the influence of the dominant peaks and their harmonics in the relevant frequency domain as well as related aliases because of the observational interruptions. We validated our prewhitening method through numerical simulations (SOM text).
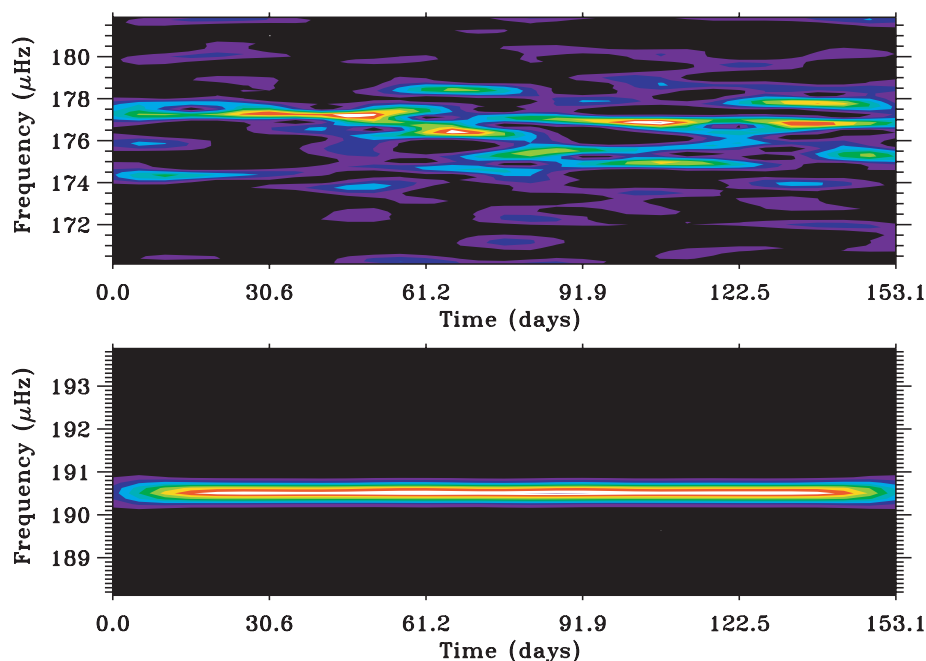
The modes associated with the broad structures have a finite lifetime, in contrast with opacity-driven modes, which are coherent oscillations and therefore appear as sinus cardinal functions in the Fourier spectrum. The amplitudes of these oscillations vary stochastically in time, again in contrast with the stationary property of the dominant opacity-driven mode and its harmonics. Their power is intermittent in time and dispersed in terms of frequency (Fig. 2). Such behavior, typical of solar-like modes (8), confirms the stochastic nature of the structures. In contrast, the temporal behavior of the second harmonic of the fundamental opacity-driven mode, which lies in the same frequency interval, is centered on a single frequency (Fig. 2, bottom). The widths of the detected high-frequency modes show that they are damped, which is a signature of modes excited by turbulent convection.

We looked for regularly spaced patterns in the Fourier spectrum, which are a characteristic signature of those modes. An autocorrelation of the Fourier spectrum shows periodicities centered around 5, 14, and 27 μHz (Fig. 3), indicating the existence of periodicities in the power spectrum.

Theoretical calculations show that these properties, interpreted as damped acoustic modes excited by turbulent convection, are compatible with solar-like oscillations of a massive main sequence star. We carried out numerical simulations using a 10–solar mass stellar model that is appropriate for V1449 Aql in that it corresponds to the observational constraints obtained from ground-based observations (9). A comparison between the theoretical and observational autocorrelations shows that the observed frequency spectrum is compatible with the presence of modes of angular degrees l = 0, 1, and 2, characterized by a large frequency separation around 27 μHz, with 1-μHz widths and a rotational splitting of 2.5 μHz related to a rotation with an axis inclined by 90° with respect to the line of sight (SOM text).

Mode amplitudes obtained from theoretical computations of the line width (10) and the energy supplied in the mode by turbulent convection (11) reach several tens of parts per million, which is well above the CoRoT detection threshold and in agreement with observations. Our calculations show that excitation by the turbulent convective motions associated with the iron-opacity bump in the upper layers of the star is efficient. This driving is operative when the convective time scale of energy-bearing eddies is close to the modal period, which explains why modes in the frequency range of 100 to 250 μHz are observed.

In summary, we showed that the broad structures at high frequencies detected in the CoRoT Fourier spectrum of the star V1449 Aql are not the result of instrumental effects, are independent of the opacity-driven modes, and present regularly spaced patterns that are characteristic of high-frequency acoustic modes. These structures have the theoretically expected properties of solar-like oscillations: modes excited by turbulent convection.



**Fig. 2.** Time-frequency diagram, using a Morlet wavelet with a 20-day width (8). (**Top**) Solar-like mode in the prewhitened light curve shown in the inset of Fig. 1, which exhibits a time-dependent behavior and a spreading over several μHz. (**Bottom**) For comparison, the second harmonic of the dominant peak, associated with the opacity-driven mode in the unprewhitened light curve.
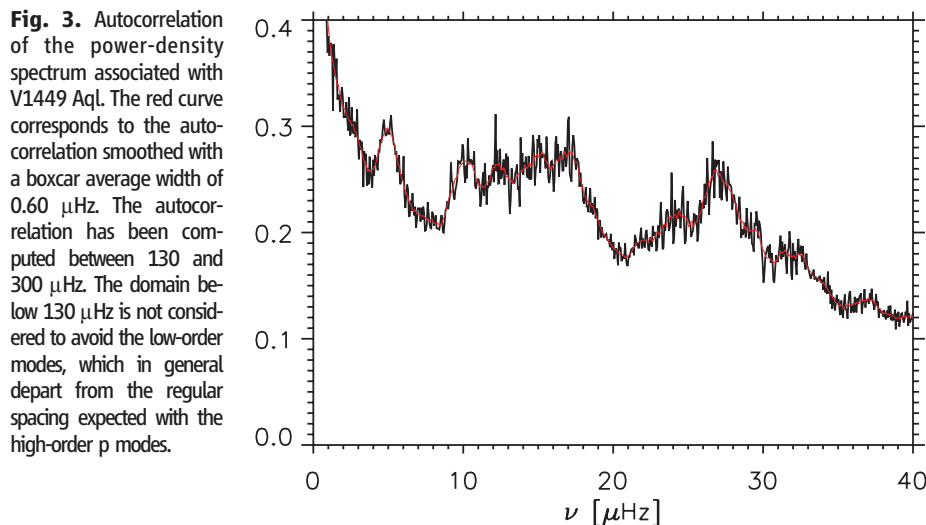


**Fig. 3.** Autocorrelation of the power-density spectrum associated with V1449 Aql. The red curve corresponds to the autocorrelation smoothed with a boxcar average width of 0.60 μHz. The autocorrelation has been computed between 130 and 300 μHz. The domain below 130 μHz is not considered to avoid the low-order modes, which in general depart from the regular spacing expected with the high-order p modes.

### References and Notes

1. C. Waelkens *et al.*, *Astron. Astrophys.* **330**, 215 (1998).
2. K. Uytterhoeven *et al.*, *J. Phys. Conf. Ser.* **118**, 012077 (2008).
3. W. A. Dziembowski, A. A. Pamiatnykh, *Mon. Not. R. Astron. Soc.* **262**, 204 (1993).
4. M. Cantiello *et al.*, *Astron. Astrophys.* **499**, 279 (2009).
5. The CoRoT space mission, launched on 27 December 2006, has been developed and is operated by CNES, with the contribution of Austria, Belgium, Brazil, the European Space Agency (ESA) (Research and Scientific Support Department and Science Programme), Germany, and Spain.
6. M. Auvergne *et al.*, *Astron. Astrophys.*, http://arXiv.org/abs/0901.2206.
7. E. Michel *et al.*, *Science* **322**, 558 (2008).
8. F. Baudin, A. Gabriel, D. Gibert, *Astron. Astrophys.* **285L**, 29 (1994).
9. T. Morel, C. Aerts, *CoAst* **150**, 201 (2007).
10. M. A. Dupret, *Astron. Astrophys.* **366**, 166 (2001).
11. K. Belkacem *et al.*, *Astron. Astrophys.* **478**, 163 (2008).
12. K.B. acknowledges financial support from Liège University through the Subside Fédéral pour la Recherche. Part of this research was funded by the Belgian Prodex-ESA. L.L. has been partly supported by CNES. A.T. is Chercheur Qualifié at the Fonds National de la Recherche Scientifique (FNRS) and A.M. is Chargé de recherches FNRS.

# Colloidal Quantum-Dot Photodetectors Exploiting Multiexciton Generation

Vlad Sukhovatkin, Sean Hinds, Lukasz Brzozowski, Edward H. Sargent*

Multiexciton generation (MEG) has been indirectly observed in colloidal quantum dots, both in solution and the solid state, but has not yet been shown to enhance photocurrent in an optoelectronic device. Here, we report a class of solution-processed photoconductive detectors, sensitive in the ultraviolet, visible, and the infrared, in which the internal gain is dramatically enhanced for photon energies $E_{photon}$ greater than 2.7 times the quantum-confined bandgap $E_{bandgap}$. Three thin-film devices with different quantum-confined bandgaps (set by the size of their constituent lead sulfide nanoparticles) show enhancement determined by the bandgap-normalized photon energy, $E_{photon}/E_{bandgap}$, which is a clear signature of MEG. The findings point to a valuable role for MEG in enhancing the photocurrent in a solid-state optoelectronic device. We compare the conditions on carrier excitation, recombination, and transport for photoconductive versus photovoltaic devices to benefit from MEG.

Multiexciton generation (MEG) refers to the creation of two or more electron-hole pairs per absorbed photon in a semiconductor (*1*). Colloidal quantum-dot materials in which MEG has been reported experimentally include PbS and PbSe (*2*), PbTe (*3*), CdSe (*4*), and Si (*5*). In bulk semiconductors, carrier multiplication has been observed repeatedly over the past five decades, both in elemental semiconductors such as germanium (*6*) and silicon (*7*) and also in lead chalcogenides (*8*), including the infrared-bandgap bulk semiconductor PbS (*9*). In the past year, experiments that carefully account for processes such as photoionization of nanoparticles during spectroscopic studies have evidenced the production of more than one exciton per photon (*10*) in colloidal quantum dots, with yields ranging from 1.1 to 2.4 excitons per photon (*10*) when the photon energy exceeds the MEG threshold near $\sim E_{photon}/E_{bandgap} > 2.7$ (*11*), where $E_{photon}$ is the photon energy and $E_{bandgap}$ is the quantum-confined bandgap.

MEG has been reported, based on all-optical spectroscopic data, not only in solution but also in thin solid films; however, in spite of numerous attempts with materials systems and photon energies reported to manifest MEG, neither the external quantum efficiency (EQE) nor the internal quantum efficiency (IQE) of the photocurrent in a device has been shown to exceed 100% (*12–20*).

In particular, one careful and systematic study (*21*) recently explored whether a key signature of MEG—an IQE of greater than unity—was observable in the photocurrent of a low-bandgap PbSe colloidal quantum-dot photovoltaic device. Once reflection and absorption were carefully taken into account, IQEs approaching, but not exceeding, 100% were reported.

Recent reports (*22*) suggest that in some of the earlier spectroscopic studies, the apparent quantum yield of MEG was enhanced by photoionization in the presence of multiple excitons. The sequence of steps is depicted in Fig. 1. The generation of two excitons within one quantum dot (Fig. 1B) produces efficient Auger recombination; one exci-

ton recombines, and one carrier associated with the other exciton is excited high within its band (Fig. 1C). Photoionization, in this instance known as Auger-assisted ionization (AAI), may occur when this excited charge carrier becomes trapped at or near the quantum dot's surface, resulting in a nanoparticle that possesses a long-lived net charge (Fig. 1D). The energetic Auger electron has a higher probability of being captured to a trap than does an already-thermalized electron (*23*) because it can more easily surmount the energetic barrier (such as a thin oxide on the nanoparticle surface), restricting access to a surface trap state.

Subsequent photogeneration of even a single exciton then results in the presence of a trion (an exciton plus a charge) that recombines rapidly, masquerading as MEG in recombination dynamics–based studies. Thus, MEG's time-resolved spectroscopic signatures are enhanced by photoionization. It should be emphasized that, at the low intensities of interest in MEG investigations, photoionization alone cannot masquerade as MEG and serves only to amplify the apparent quantum yield if MEG is already present.

Unfortunately, MEG combined with photoionization provides no advantages over MEG alone in the harvest of photovoltaic energy. Indeed, because trions resulting from photoionization accelerate recombination, they render even more challenging the extraction of MEG photocurrent from a photovoltaic device. To observe the benefits of MEG in the current extracted from a photovoltaic device, charge separation must occur before
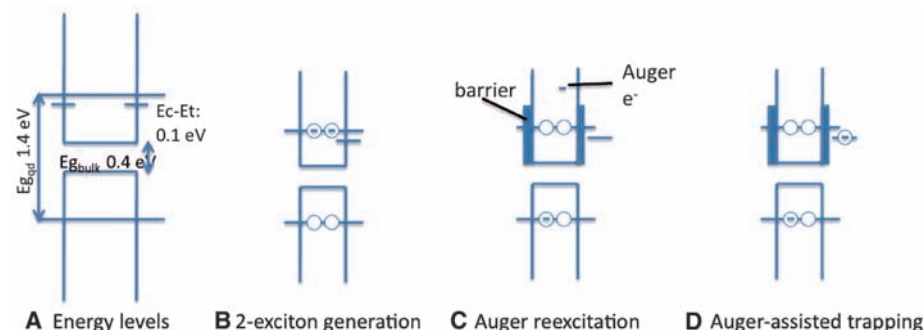
Department of Electrical and Computer Engineering, University of Toronto, Toronto, ON M5S 3G4, Canada.

*To whom correspondence should be addressed. E-mail: ted.sargent@utoronto.ca

**Fig. 1.** MEG accompanied by photoionization. (**A**) Bands and trap levels for the quantum dots that were used. $E_c$ is the quantum-confined conduction band edge, $E_t$ is the trap energy, $E_{gqd}$ is the quantum-confined bandgap, and $E_{gbulk}$ is the constituent semiconductor's bulk bandgap. (**B**) Generation of a pair of excitons via photon absorption followed by carrier multiplication. (**C**) Auger-induced excitation of an electron to a higher-lying level concomitant with recombination of the other exciton. (**D**) Efficient trapping of the excited electron.